Design of 4 × 4 and 8 × 8 filtering butler matrices utilizing combined 90° and 180° couplers

Shao, Qiang; Chen, Fu Chang; Wang, Yi; Chu, Qing Xin

DOI:
10.1109/TMTT.2021.3085879

Document Version
Peer reviewed version

Citation for published version (Harvard):
Shao, Q, Chen, FC, Wang, Y & Chu, QX 2021, 'Design of 4 × 4 and 8 × 8 filtering butler matrices utilizing combined 90° and 180° couplers', *IEEE Transactions on Microwave Theory and Techniques*, vol. 69, no. 8, pp. 3842-3852. https://doi.org/10.1109/TMTT.2021.3085879

Design of 4 × 4 and 8 × 8 Filtering Butler Matrices Utilizing Combined 90° and 180° Couplers

Qiang Shao, Fu-Chang Chen, *Member*, *IEEE*, Yi Wang, *Senior Member*, *IEEE* and Qing-Xin Chu, *Fellow*, *IEEE*

***Abstract*—In this paper, a novel design approach for designing 4 × 4 and 8 × 8 filtering Butler matrices is proposed. The matrices, composed of combined 90° couplers and 180° filtering couplers as well as phase shifters, provide incremental phase shifts and a bandpass filter performance. The detailed design process and synthesis method for the Butler matrices are presented. A three-layer symmetrical stripline structure is used to realize the Butler matrix, allowing a fully planar structure without interlayer connections. For experimental verification, two prototype 4 × 4 and 8 × 8 filtering Butler matrices, operating at the center frequency of 2.4 GHz with a bandpass response, are devised, manufactured, and tested. The test results match well with the simulation ones. Based on the measurements, array factors have been calculated, which further indicate the acceptance of the measured results.**

***Index Terms*—Bandpass filter, Butler matrix, stripline, 90° couplers, 180° couplers.**

I. Introduction

MULTI-BEAM antenna array has attracted much attention over the recent years because of its higher spectral efficiency and larger communication capacity. A classic multi-beam antenna array is usually comprised of three parts with different functions: the antenna array, a beam-forming network (BFN), and switches [1]. First, the input port of BFN can be decided by using the switches. Then the input signal pass through the BFN and different phase increment can be generated at its outputs, depending on the selected input port. At last, the output signal with phase increment would feed the antenna array. The BFN is the most important part in a multi-beam antenna array system. Apart from the Blass matrix [2], which is rarely used and a lossy network, there exist two types of commonly used BFNs. One is the Nolen matrix [3]. In [4]-[6], the authors have presented several high-performance Nolen matrices. The other one is the Butler matrix [7], and some high-performance Butler matrices have been presented for the applications of multi-beam antenna array system [8]-[19]. However, in practical application, for a narrowband environment, extra bandpass filter should always be connected with the system, in order to restrain the undesired frequencies produced by the system. In this paper, we integrated the Butler matrix with extra bandpass filter as a new filtering Butler matrix, which could achieve the miniaturization of the system [20], [21].

In general, the Butler matrix is composed of couplers and phase shifters and the detailed design process has been presented in [22], [23]. The 90° coupler, which is a 2 × 2 network with a 90° phase progression between the two outputs [24], is the most frequently used in Butler matrix. Instead of 90° couplers, 180° couplers could also be used, as proposed in [25]. Since the couplers are the key component of the Butler matrix, it is plausible to first introduce filtering functions into the couplers and then use these couplers to design the filtering Butler matrix. Several filtering couplers have been proposed previously [26]-[33]. In [20], a novel filtering Butler matrix based on 180° filtering couplers was presented, in view of the application in multi-port power amplifiers.

The authors demonstrated the 2 × 4 and 4 × 6 filtering Butler matrices utilizing coupled-resonator structures in the previous work [21], [34]. However, because the filtering couplers are cascaded by the couplings between resonators, it was difficult to generate a 90° or other phase shift for the all-resonator network, which limited the number of phase increments for filtering Butler matrix within 4. The novelty in this paper lies in the utilization of combined 90° and 180° couplers so as to solve the problem of generating phase shifters in the connecting network, which innovates the realization of filtering Butler matrix with 8 phase increments for the first time. In this paper, a 4 × 4 and an 8 × 8 filtering Butler matrix are presented using both 90° and 180° couplers. The detailed synthesis process for the Butler matrices is presented, and two prototypes are devised, manufactured, and measured, achieving an equal amplitude signal distribution and multiple phase increments between the adjacent output ports.

The rest of this paper is arranged as follows. In Section II, the design process of the 4 × 4 filtering Butler matrix is presented in detail. A novel 8 × 8 filtering Butler matrix based on 90° and 180° couplers is demonstrated in Section III. Lastly, Section IV gives a conclusion for this paper.

Manuscript received January 26, 2021; revised March 12, 2021; accepted May 11, 2021. This work was supported in part by the Guangdong Provincial Key R&D Programme under Grant 2020B010179002, in part by the National Natural Science Foundation of China under Grant 62022035, and in part by the Guangdong Natural Science Funds for Distinguished Young Scholars under Grant 2019B151502032.

Q. Shao was with School of Electronics, Electrical and Systems Engineering, the University of Birmingham. He is now with the School of Electronic and Information Engineering, South China University of Technology, Guangzhou, China. F. C. Chen and Q. X. Chu are with the School of Electronic and Information Engineering, South China University of Technology, Guangzhou, China. Y. Wang is with School of Electronics, Electrical and Systems Engineering, the University of Birmingham. (e-mail: chenfuchang@scut.edu.cn).

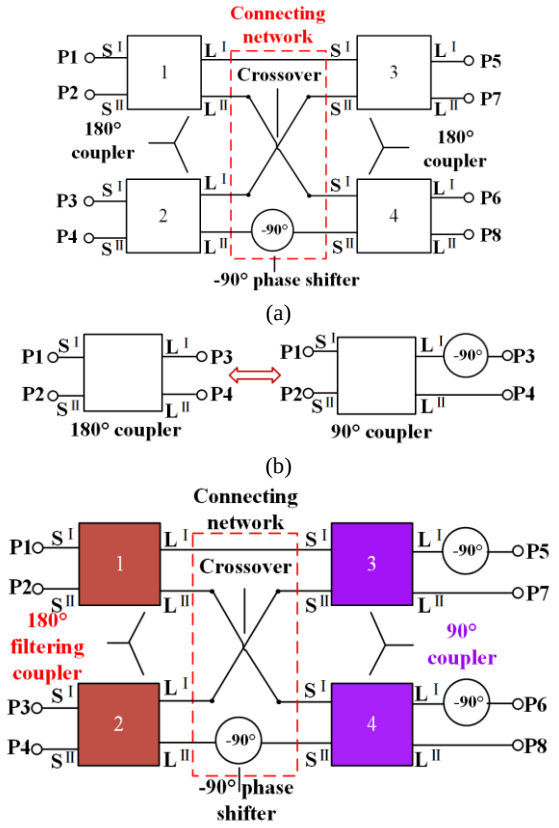

Fig. 1. (a) Diagram of the traditional 4 × 4 Butler matrix using 180°couplers. (b) The equivalence between 90° and 180° coupler. (c) Diagram of 4 × 4 filtering Butler matrix using both 90° and 180° couplers.

II. 4 × 4 Filtering Butler Matrix Using Both 90° and 180° Couplers

A. Analysis

Fig. 1(a) shows the conventional topology of a 4 × 4 Butler matrix based on 180° couplers, which can provide phase increments of 0°, 180°, and ±90°. On the one hand, to introduce the filtering characteristic into the Butler matrix, the couplers 1 and 2 are replaced by the 180° filtering couplers. On the other hand, the couplers 3 and 4 are replaced by the common 90° couplers plus an additional phase shifter as shown in Fig. 1(b). In this way, a new configuration of 4 × 4 Butler matrix with using both 90° and 180° couplers is shown in Fig. 1(c). Because the 90° coupler is not composed of coupled resonators, now the output ports of the 180° filtering coupler and the input ports of the 90° coupler can be connected directly by transmission lines, which makes it easy to implement the phase shifters in the connecting network.

In addition, because the transformations of couplers are equivalent, the phase increments between the adjacent output ports remains unchanged and can be expressed as

$$\begin{aligned}
&\angle S_{81}-\angle S_{71}=\angle S_{71}-\angle S_{61}=\angle S_{61}-\angle S_{51}=0^\circ\\
&\angle S_{82}-\angle S_{72}=\angle S_{72}-\angle S_{62}=\angle S_{62}-\angle S_{52}=180^\circ\\
&\angle S_{83}-\angle S_{73}=\angle S_{73}-\angle S_{63}=\angle S_{63}-\angle S_{53}=-90^\circ\\
&\angle S_{84}-\angle S_{74}=\angle S_{74}-\angle S_{64}=\angle S_{64}-\angle S_{54}=90^\circ
\end{aligned} \tag{1}$$

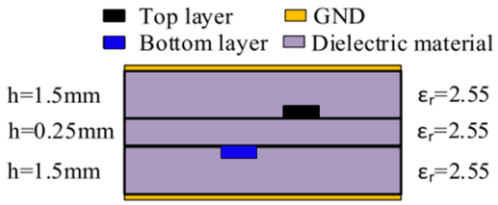

Fig. 2. A three-layer symmetrical stripline structure.

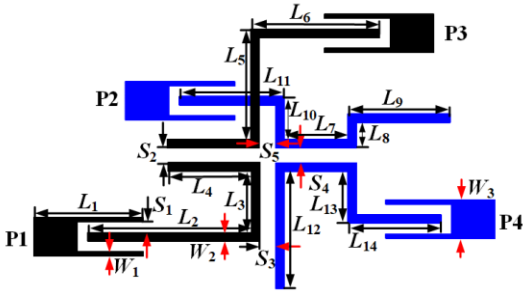

Fig. 3. Layout of the 180° filtering coupler.

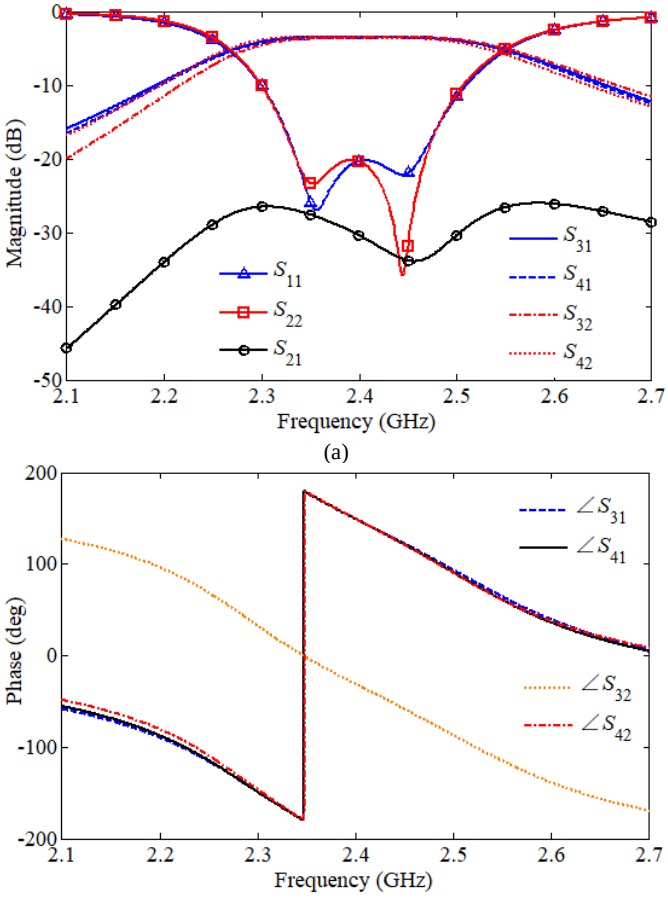

Fig. 4. Simulated *S*-parameters and output phases of the 180° filtering coupler. (a) S_{11}, S_{21}, S_{31}, S_{41}, S_{22}, S_{32} and S_{42}. (b) $\angle S_{31}$, $\angle S_{41}$, $\angle S_{32}$ and $\angle S_{42}$.

Different from our previous work [21][34], the filtering function of the new 4 × 4 Butler matrix is realized solely by the 180° filtering couplers but not the 90° couplers. The design of the 180° filtering coupler and the 90° coupler will be discussed next.

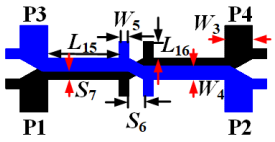

Fig. 5. Layout of the 90° directional coupler.

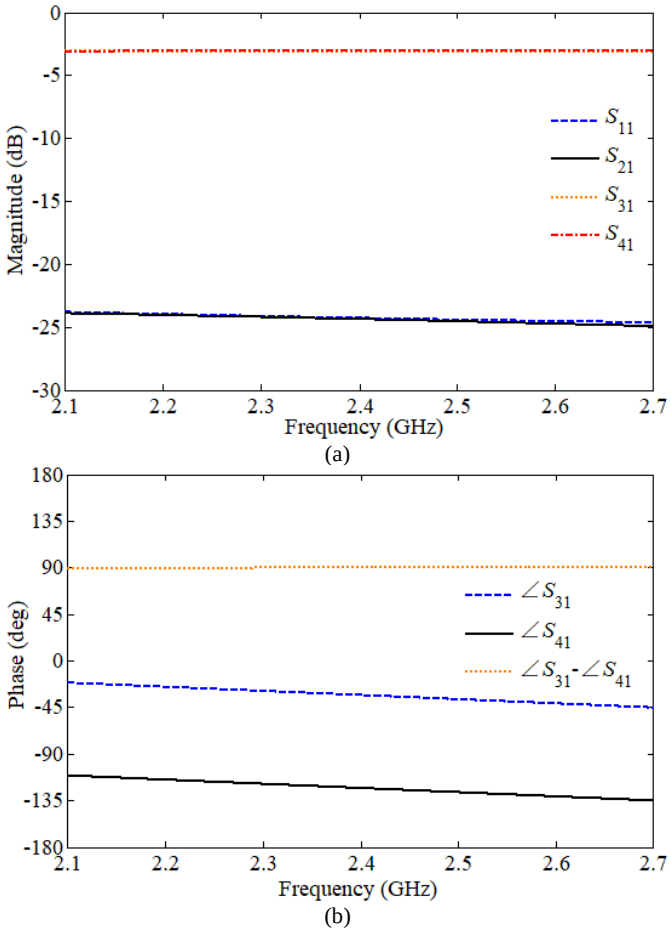

Fig. 6. Simulated *S*-parameters and output phases of the 90° directional coupler. (a) S_{11}, S_{21}, S_{31} and S_{41}. (b) $\angle S_{31}$, $\angle S_{41}$ and $\angle S_{32}$-$\angle S_{42}$.

B. 180° Filtering Coupler

The 180° filtering coupler is designed based on the method in our previous work [21]. However, a new transmission media based on a multi-layer structure is used here, as shown in Fig. 2. This three-layer stripline structure, consisting of one thin and two thick dielectric layers with the dielectric constant of 2.55, offers more design freedoms for the crossovers and couplers. Fig. 3 shows the layout of a 180° filtering coupler, consisting of four coupled resonators. Two of them are placed in the top layer of the stripline and the other two in the bottom layer. The bandpass filter is designed to operate at a center frequency f_0 = 2.4 GHz with a fractional bandwidth (*FBW*) of 5.5%. The passband ripple level is chosen to be 0.04321 dB with respect to a 20 dB return loss. Using the design method in [21], the final parameters of the coupler after optimization in Zeland IE3D software are L_1 = 13.99, L_2 = 18.79, L_3 = 7.00, L_4 = 9.58, L_5 = 12.60, L_6 = 14.83, L_7 = 7.28, L_8 = 2.88, L_9 = 11.75, L_{10} = 4.88, L_{11} = 12.05, L_{12} = 13.40, L_{13} = 5.96, L_{14} = 10.72, W_1 = 0.5, W_2 = 1.0, W_3 = 2.4, S_1 = 0.20, S_2 = 0.78, S_3 = 1.23, S_4 = 0.72, S_5 = 0.88, unit in mm. Fig. 4 shows the simulation results of *S*-parameters and output phases for the coupler. The coupler shows a 2nd-order filtering characteristic and expected phase response in the passband.

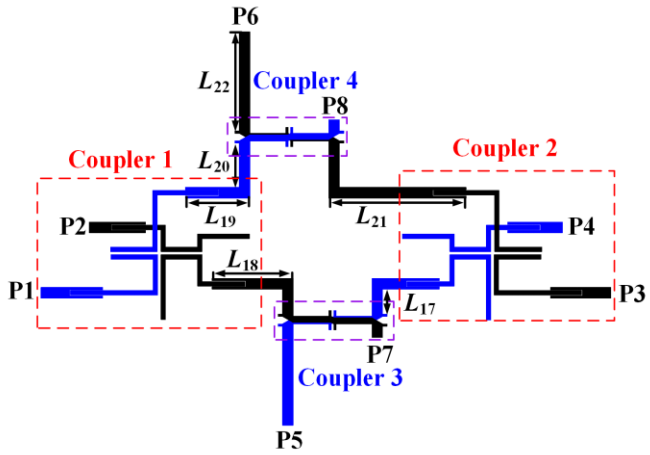

Fig. 7. Layout of the 4 × 4 filtering Butler matrix.

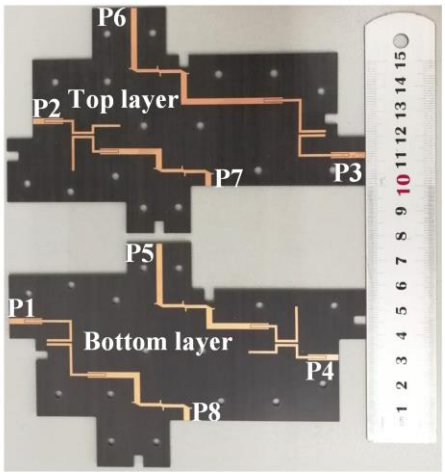

Fig. 8. Photo of the 4 × 4 filtering Butler matrix.

C. 90° Directional Coupler

The 90° directional coupler follows a design from [35] and its layout is shown in Fig. 5. Utilizing the odd–even mode analysis approach in [24], when the length of the coupled line keeps the same, the coupled port (P3 in Fig. 5) and the straight through port (P4 in Fig. 5) have a phase increment of 90° over a broadband range. The bandwidth is selected to be 2.1–2.7 GHz and the even/odd mode characteristic impedances for the coupled line are acquired as Z_{oe} = 120.4 Ω and Z_{oo} = 16.7 Ω. The parameters of the coupler in Fig. 5 can be optimized in Zeland IE3D software. They are L_{15} =8.14, L_{16} = 0.50, S_6 = 0.60, S_7 = 0.35, W_4 = 1.35, W_5 = 0.5, unit in mm. Fig. 6 shows the simulation results of *S*-parameters and output phases for the coupler. The simulated results show the coupler has balanced amplitude and phase response over the range of 2.1–2.7 GHz.

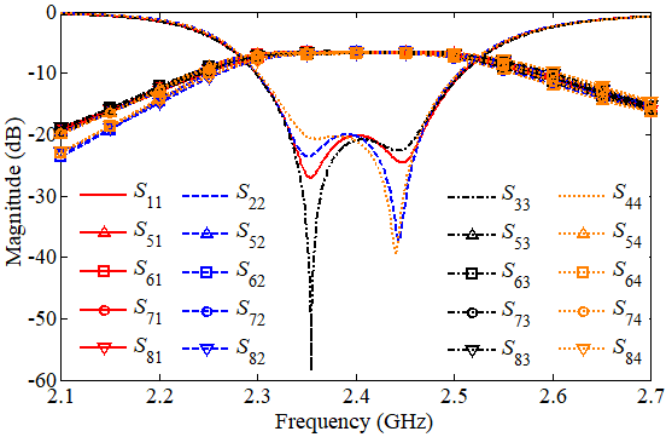

(a)

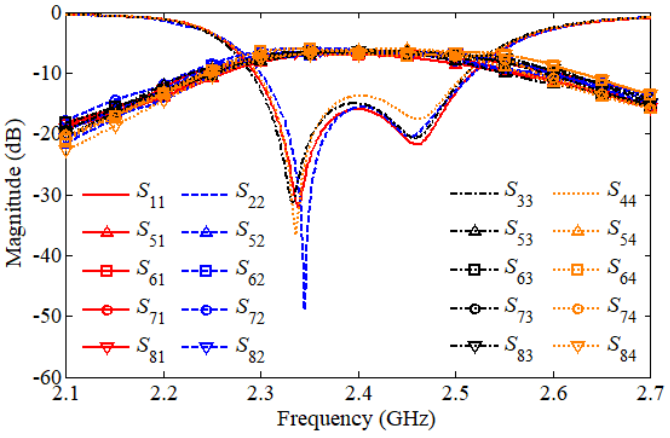

(b)

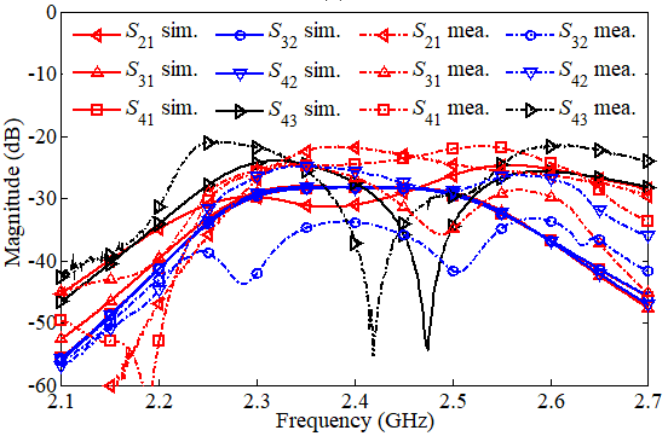

(c)

Fig. 9. Simulation and test results for the manufactured 4 × 4 filtering Butler matrix. (a) Simulated *S*-parameters. (b) Measured *S*-parameters. (c) Simulated and measured isolations between the input ports.

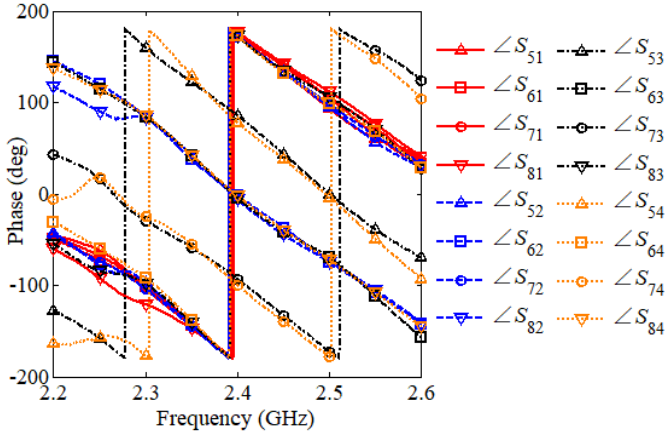

(a)

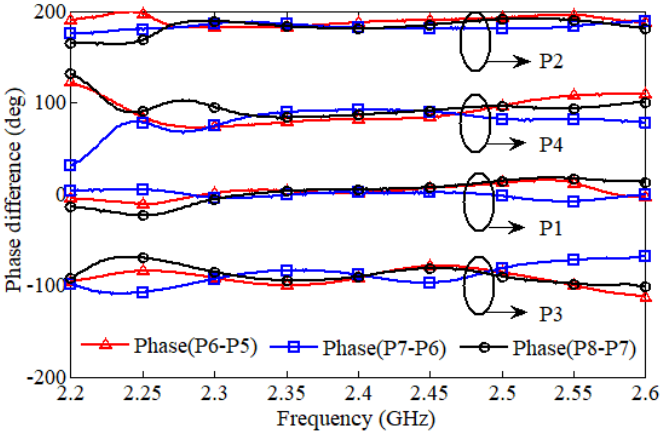

(b)

Fig.10. Measurement results for the manufactured 4 × 4 filtering Butler matrix. (a) Output phases. (b) Phase differences.

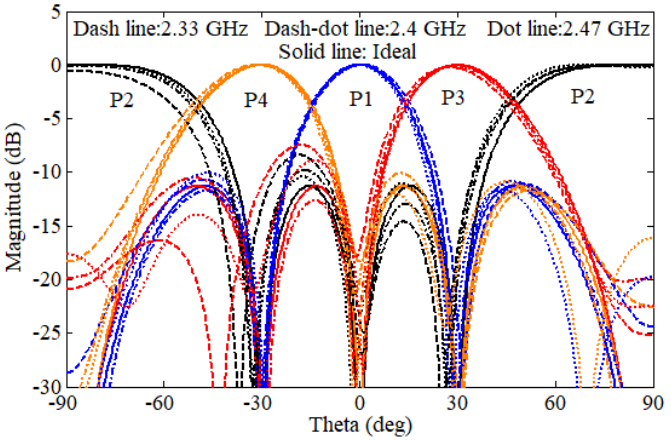

Fig. 11. Theoretical and calculated normalized array factors for the four-element linear antenna array by using ideal and measured results.

D. Butler Matrix Simulations and Measurements

Based on the topology in Fig. 1(c), a 4 × 4 filtering Butler matrix is obtained by connecting the couplers with striplines. Fig. 7 presents the layout of the 4 × 4 filtering Butler matrix and a photo of the manufactured Butler matrix is given in Fig. 8. The parameters of the connecting network in Fig. 7 can be optimized to be L_{17} =5.56, L_{18} = 25.37, L_{19} = 21.64, L_{20} = 9.87, L_{21} = 41.12, L_{22} = 22.07, unit in mm. Fig. 9(a) and (b) show the simulation and test results of *S*-parameters when different input port is excited. The test results have a good consistency with the simulation ones. The measured insertion loss in the passband is 6.7±0.7dB, which includes 6 dB power distribution loss. The measured return losses in the passband are above 13 dB. This small difference from the simulation results is mainly attributed to the assembling errors from the multi-layer structures. Fig. 9(c) shows the simulation and test results of isolation between the input ports. The measured isolation between the input ports is better than 21 dB. Fig. 10(a) and (b) show the measurement results of output phases and

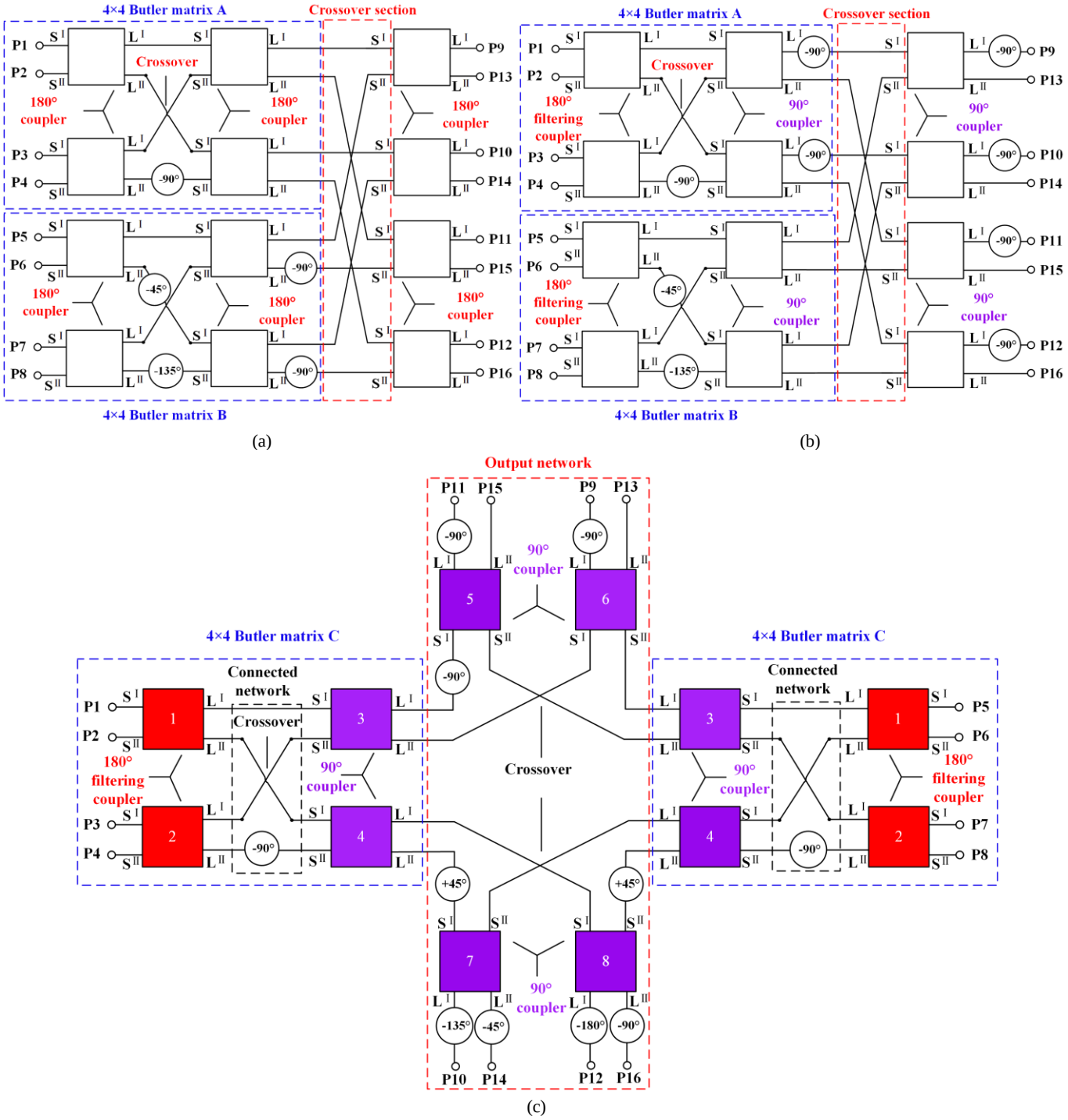

Fig. 12. (a) Topology of the traditional 8 × 8 Butler matrix using 180° couplers. (b) Topology of the 8 × 8 filtering Butler matrix using both 90° and 180° couplers. (c) Topology of the proposed new 8 × 8 filtering Butler matrix consisting of two 4 × 4 filtering Butler matrices and the output network.

phase differences for the Butler matrix, respectively. For the input port P1 to P4, it is easy to find that the measured phase differences between the adjacent output ports in the passband are 0°, 180° and ±90°. The measured output phase imbalances of filtering Butler matrix are within ± 10° in the passband. It is worth mentioning that the filtering function of the 4 × 4 filtering Butler matrix is introduced by the 180° filtering coupler. Therefore, the filter order could be easily extended by cascading more resonators at the input or output ports of the 180° filtering coupler.

In order to further verify the acceptance of the measured results, the normalized array factors of an linear antenna array with four elements have been calculated by using the measured phases and amplitudes of the 4 × 4 filtering Butler matrix. Fig. 11 shows the theoretical and calculated array factors for the center frequency f_0 = 2.4 GHz with radiating elements' spacing equal to $0.5\lambda_0$. Close correlation has been found between the calculated array factors and the theoretical ones.

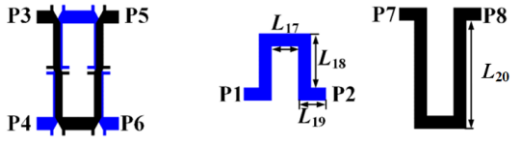

(a) (b)

Fig. 13. Layout of the connecting network. (a) Crossover. (b) Phase compensator.

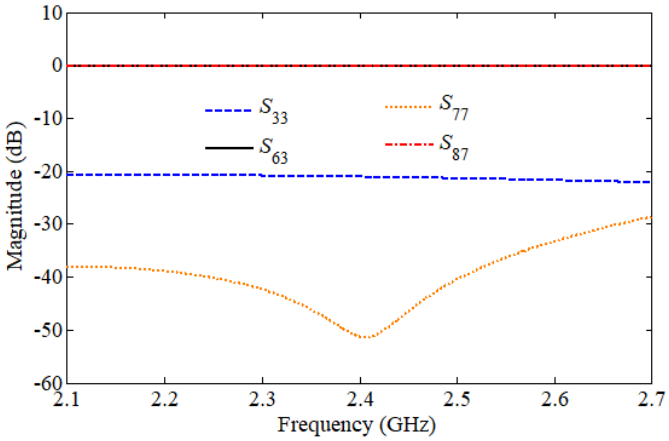

(a)

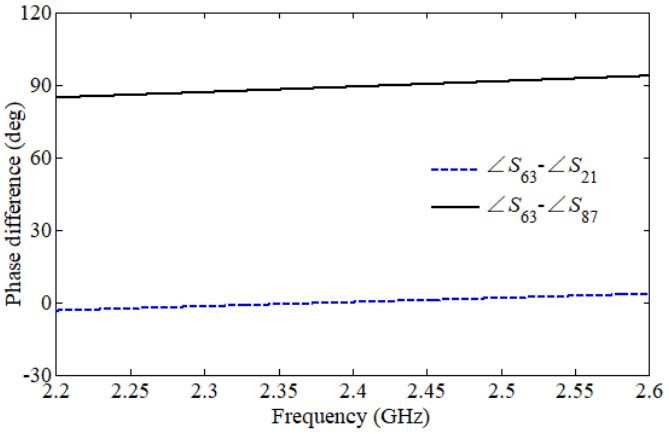

(b)

Fig. 14. Simulation results of the connecting network. (a) Magnitude. (b) Phase difference.

TABLE I
PHASE DISTRIBUTION OF THE 4 × 4 FILTERING BUTLER MATRIX C

	P5	P6	P7	P8
P1	0°	0°	-90°	-90°
P2	0°	-180°	-90°	-270°
P3	-90°	-180°	0°	-90°
P4	-90°	0°	0°	-270°

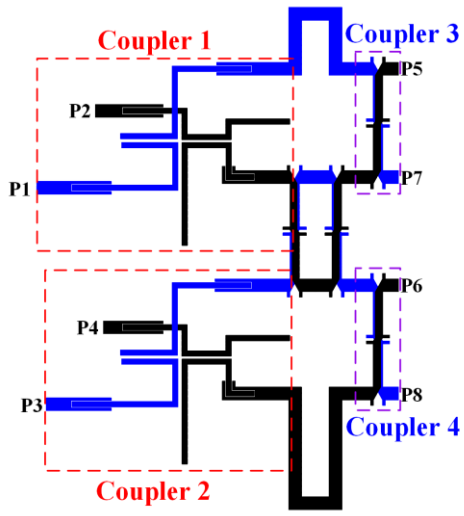

(a)

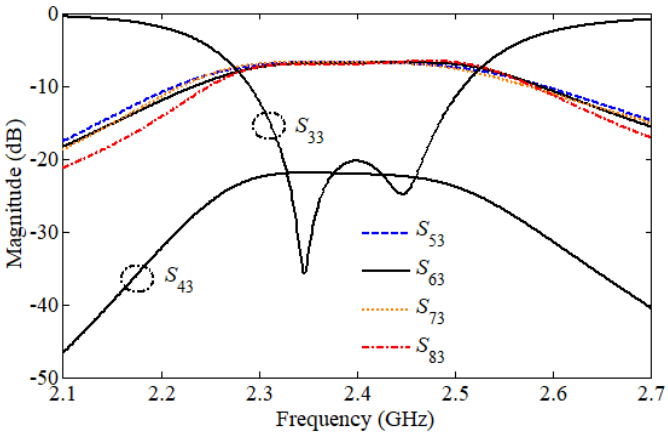

(b)

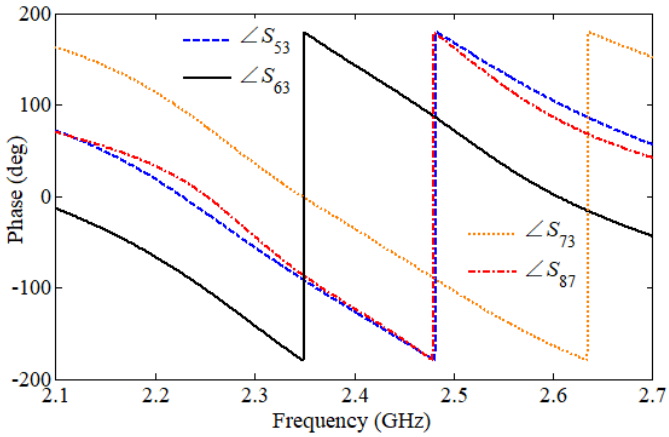

(c)

Fig. 15. (a) Layout of the 4 × 4 filtering Butler matrix C. Simulation results of the 4 × 4 filtering Butler matrix C. (b) Magnitude. (c) Output phases.

III. 8 × 8 FILTERING BUTLER MATRIX USING BOTH 90° AND 180° COUPLERS

A. Analysis

Based on the 4 × 4 filtering Butler matrix, a method for designing an 8 × 8 filtering Butler matrix is described in this section. Fig. 12(a) shows the topology of a conventional 8 × 8 Butler matrix using 180° couplers, with phase progressions of 0°, ±45°, ±90°, ±135°, and 180°. The 8 × 8 Butler matrix is composed of two 4 × 4 Butler matrices A and B and four 180° couplers. They are connected by crossover sections. Since the realization of a filtering Butler matrix is of interest, the 180° couplers connected with input ports are replaced by 180° filtering couplers, introducing filter functions into the Butler matrix. The other 180° couplers are replaced by 90° couplers and additional phase shifts. Fig. 12(b) shows the topology of an 8 × 8 filtering Butler matrix using both 90° and 180°

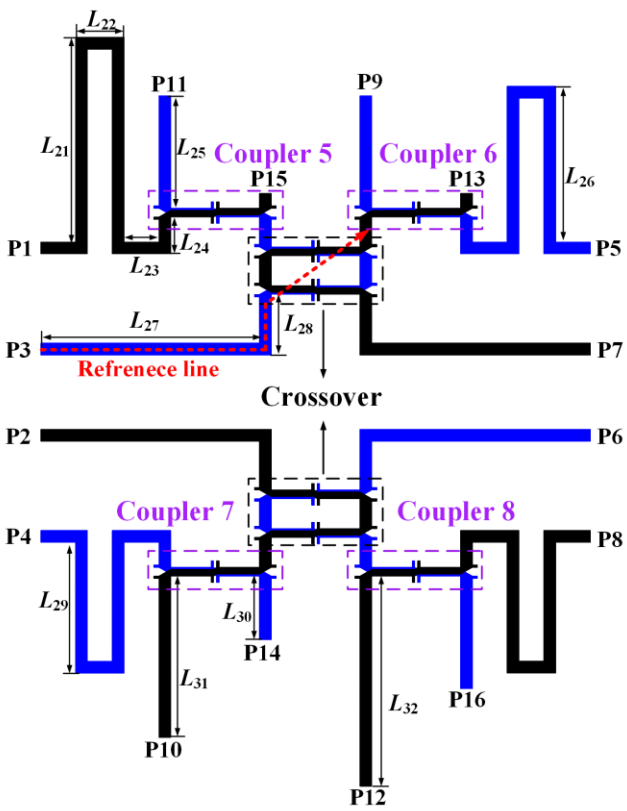

Fig. 16. Layout of the output network for the 8 × 8 Butler matrix.

TABLE II
PHASE DISTRIBUTION OF THE OUTPUT NETWORK IN FIG. 16

	P9	P10	P11	P12	P13	P14	P15	P16
P1			-180°				-180°	
P2				-180°				-180°
P3	-90°				-90°			
P4		-90°				-90°		
P5	-180°				0°			
P6		-225°				-45°		
P7			-180°				0°	
P8				-225°				-45°

couplers. In order to simplify the 8 × 8 filtering Butler matrix and make it easier to be integrated as a planar structure, the crossover section is rearranged, and the phase shifters are adjusted. This leads to a new topology as shown in Fig. 12(c). Noted that the number of crossovers is reduced from six to four compared with the topology used in [19]. The new 8 × 8 filtering Butler matrix could be divided into two parts: the filtering 4 × 4 Butler matrix C and the output network, which can be designed as followed.

B. Filtering 4 × 4 Butler Matrix C

The same design method as described in Section II is used. The filter is still operating at 2.4 GHz with a *FBW* of 5.5% and a 20 dB return loss. The design of the 90° and 180° couplers keeps the same. The crossover in the filtering 4 × 4 Butler matrix C is realized by a tandem connection of two 90° directional couplers. This is regarded the reference line. The -90° phase shifter is realized by adding additional quarter-

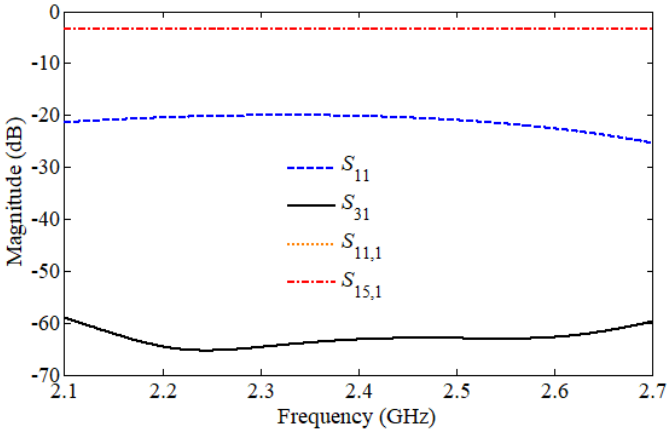

(a)

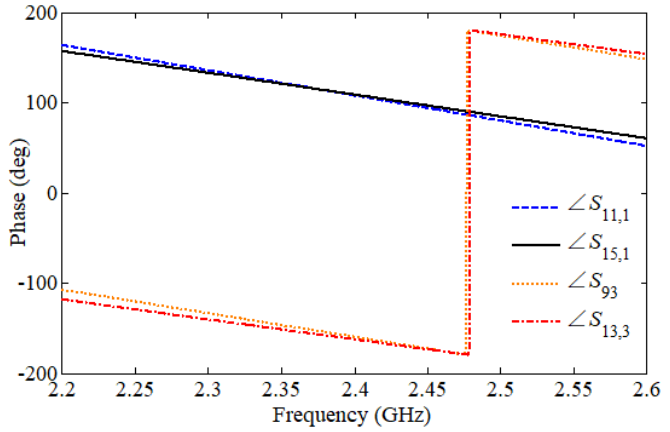

(b)

Fig. 17. Simulated *S*-parameters and output phases of the output network. (a) S_{11}, S_{31}, $S_{11,1}$ and $S_{15,1}$. (b) $\angle S_{11,1}$, $\angle S_{15,1}$ $\angle S_{93}$ and $\angle S_{13,3}$.

wavelength stripline on top of the reference line. Fig. 13(a) and (b) show the layout of the connecting network of the filtering 4 × 4 Butler matrix C. By properly adjusting the length of the striplines (L_{18} and L_{20}), the phase difference between the different path can be easily controlled. The parameters of the connecting network after optimization in IE3D software are L_{17} = 5.2, L_{18} = 10.3, L_{19} = 5.3, L_{20} = 20.56, unit in mm. Fig. 14(a) and (b) show the simulation and test results of *S*-parameters and output phase differences for the connecting network. The simulated phase imbalances between different paths are within ±5° in the range of 2.2–2.6 GHz. The 4 × 4 filtering Butler matrix C is obtained by connecting the couplers with the connecting network directly. The layout of the 4 × 4 filtering Butler matrix C is given in Fig. 15(a). From the topology of the 4 × 4 filtering Butler matrix C in Fig. 12(c), Table I shows the phase distributions from each input port to output port for the Butler matrix C. Fig. 15(b) and (c) show the simulation and test results of S-parameters and output phases for the 4 × 4 filtering Butler matrix C when the input port P3 is excited. As can be observed from the simulated results, the 4 × 4 filtering Butler matrix C has 2nd-order filtering characteristic and its output phase increments across the output ports are -90°, 180° and -90°, which are consistent with the theoretical phase distribution in Table I.

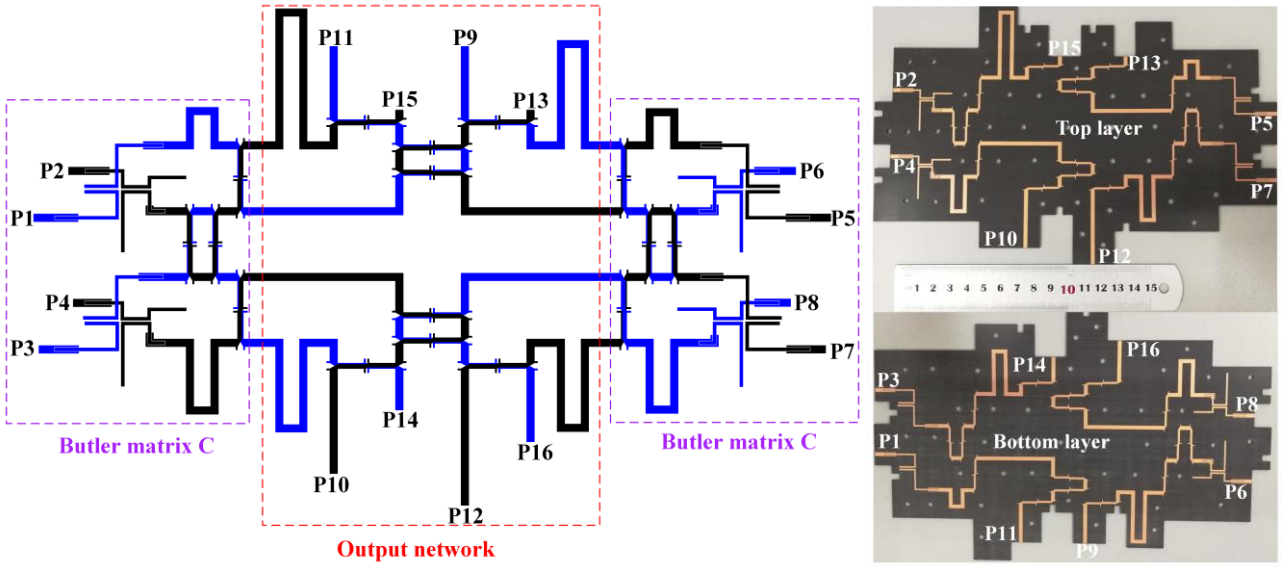

(a) (b)

Fig. 18. (a) Layout of the 8 × 8 filtering Butler matrix. (b) Photograph of the 8 × 8 filtering Butler matrix.

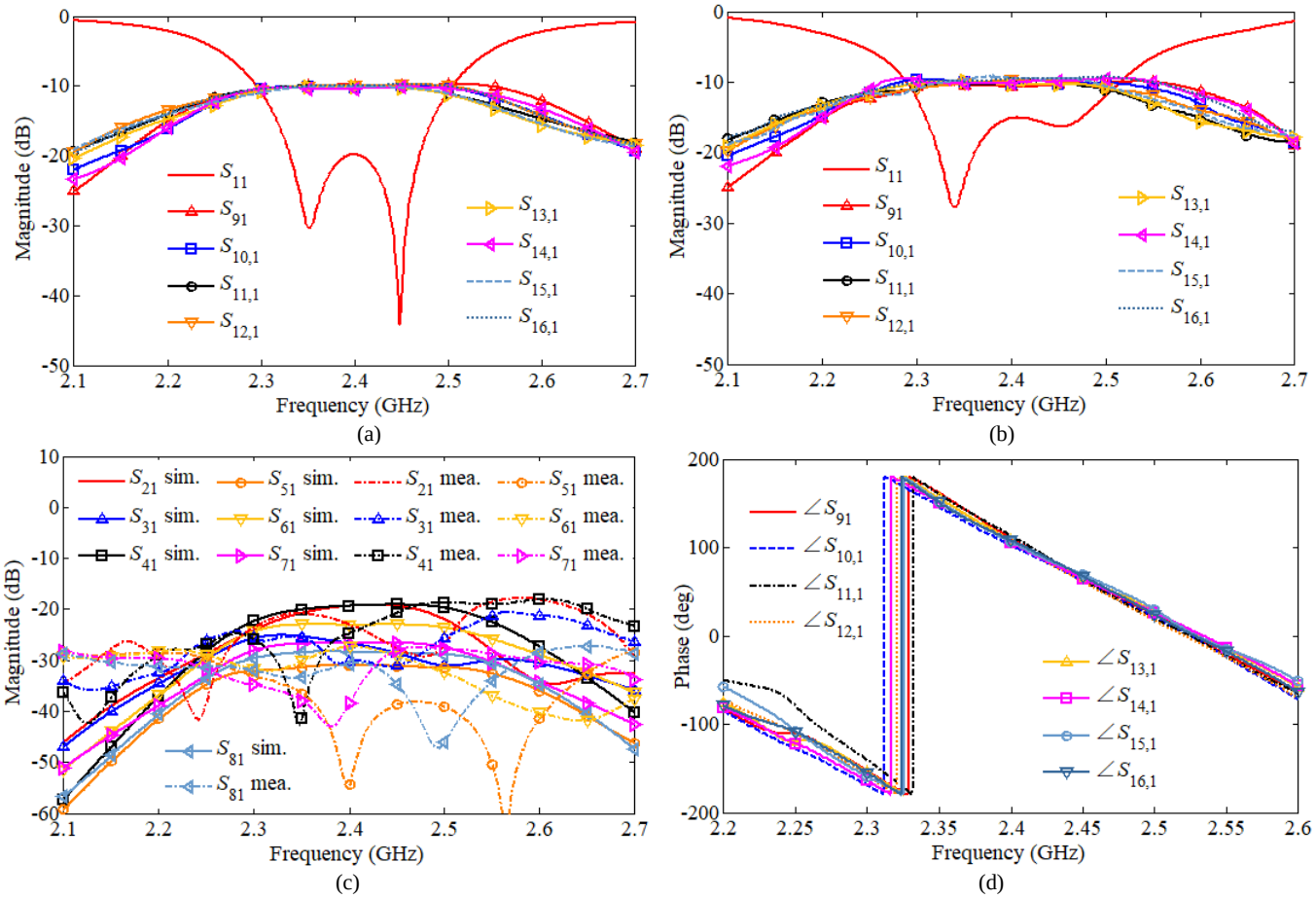

Fig. 19. Simulation and test results for the filtering 8 × 8 Butler matrix when port P1 is excited. (a) Simulated *S*-parameters. (b) Measured *S*-parameters. (c) Simulated and measured isolations between the input ports. (d) Measured output phase.

C. Output network

The layout of the output network is shown in Fig. 16. From the output network in Fig. 12(c), Table II shows the phase distributions from each input port to output port for the output network. The crossover is still realized by a tandem connection of two 90° directional couplers. For the -90° and +45° phase shifters connected with the input port of the 90° directional couplers, taking the crossover path as the reference line, additional quarter-wavelength and one-eighth-wavelength stripline should be added and deducted, respectively. By properly adjusting the length of the striplines (L_{21} and L_{29}),

TABLE III
MEASURED RESULTS FOR THE FILTERING 8 × 8 BUTLER MATRIX

	RL (dB)	IL (dB)								Iso (dB)
		P9	P10	P11	P12	P13	P14	P15	P16	
P1	15	10.6	10.3	10.1	9.8	10.4	10.1	9.5	9.6	>19
P2	14	10.3	10.4	9.9	10.1	10.2	10.4	9.8	10.2	>19
P3	16	10.5	10.3	10.2	10.2	10.0	10.2	10.2	10.0	>17
P4	17	10.3	10.2	10.0	9.9	9.9	9.9	10.2	9.9	>17
P5	20	10.5	10.2	10.2	10.1	10.3	9.8	9.9	9.7	>17
P6	14	10.2	10.1	10.3	10.2	10.1	10.1	9.8	10.1	>17
P7	16	10.4	10.3	9.9	9.8	10.5	10.2	10.2	10.4	>18
P8	15	10.3	10.3	9.8	10.1	10.2	10.3	10.1	10.2	>18

RL: Return loss; IL: Insertion loss; Iso: Isolation.

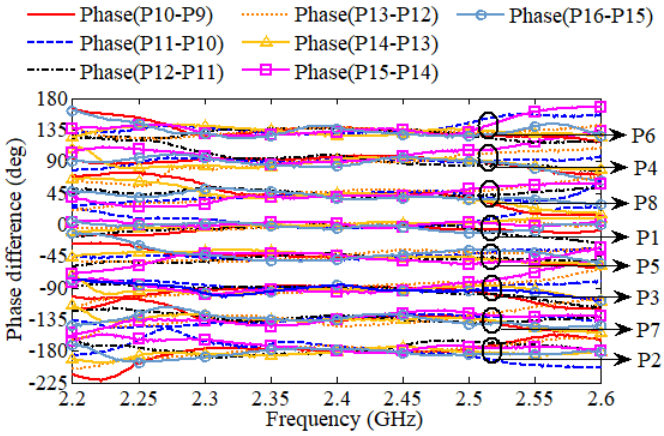

Fig. 20. Measured phase differences for the manufactured 8 × 8 filtering Butler matrix.

these phase shifters can be easily realized. For the -45°, -90°, -135° and -180° phase shifters connected with the output port of the 90° directional couplers, additional one-eighth-wavelength, quarter-wavelength, three-eighth-wavelength and half-wavelength striplines are added to the output ports. The parameters of the output network in Fig. 16 can be optimized in IE3D software to be L_{21} =41.02, L_{22} = 9.8, L_{23} = 7.0, L_{24} = 7.4, L_{25} = 22.55, L_{26} = 31.2, L_{27} = 46.48, L_{28} = 12.16, L_{29} = 26.48, L_{30} = 12.77, L_{31} = 32.34, L_{32} = 42.13, unit in mm.

Fig. 17 shows the simulation and test results of *S*-parameters and output phases for the output network when the input port P1 is excited. It can be observed from the simulated results that the output phases $\angle S_{11,1}$ and $\angle S_{15,1}$ ($\angle S_{93}$ and $\angle S_{13,3}$) are equal and the output phase difference between $\angle S_{11,1}$ and $\angle S_{93}$ is -90°, which are consistent with the phase distribution given in Table II.

D. Butler Matrix Simulations and Measurements

An 8 × 8 filtering Butler matrix is obtained by connecting the 4 × 4 filtering Butler matrix C with the output network according to Fig. 12(c). The entire layout of the 8 × 8 filtering Butler matrix is given in Fig. 18(a). Fig. 18(b) shows a photo of the manufactured filtering Butler matrix. Fig. 19(a) and (b) show the simulation and test results of *S*-parameters when the port P1 is excited, respectively. Small difference has been found between the test results and simulation ones. The measured insertion loss in the passband is 10.2±0.7 dB, which includes 9 dB power distribution. The measured return losses in the passband are above 15 dB. Fig. 19(c) shows the

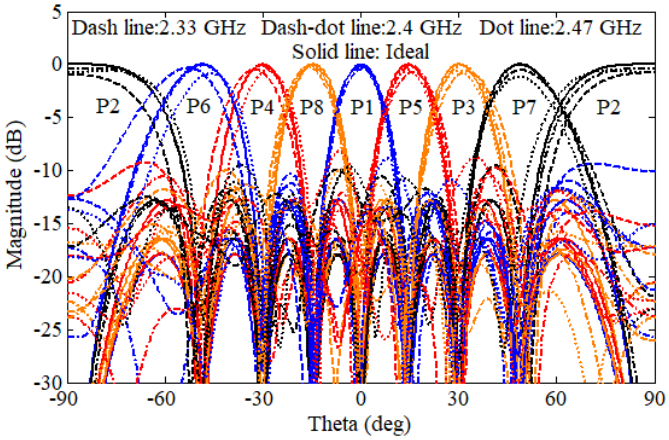

Fig. 21. Theoretical and calculated normalized array factors for the eight-element linear antenna array by using ideal and measured results.

TABLE IV
COMPARISON WITH PREVIOUS WORK

Ref.	Number of phase increments	Filtering function	Technology	Type of realized couplers	IL (dB)	PI (deg)	f_0 (GHz)	*FBW* (%)
[13]	8	No	CMOS	90° coupler	3.1	±22	60	16.6
[16]	8	No	Stripline	90° coupler	1	±10	3	33
[20]	0	Yes	3D printing	180° coupler	NG	NG	12.4	4
[21]	2	Yes	Microstrip	180° coupler	2.8	± 9	2.4	3.5
[34]	4	Yes	Microstrip	180° coupler	2.9	±10	2.4	8
This work	**8**	**Yes**	**Stripline**	**90° and 180° couplers**	**1.9**	**±12**	**2.4**	**5.5**

IL: Insertion loss; PI: Phase imbalance; NG: Not given.

simulated and measured isolations between the input ports when port P1 is excited. The measured isolation between the input ports is better than 19 dB. Fig. 19(d) shows the measurement results of output phases for the Butler matrix when the input port P1 is excited. It is easy to find that the output phases from $\angle S_{91}$ to $\angle S_{16,1}$ are almost equal. Table III lists the measured return loss, insertion loss and isolation between the input ports when other ports are excited. Fig. 20 shows the measured phase differences when different port is excited. It can be concluded from the figure that when other input ports are excited, the measurement results of phase increment are 180°, ±90°, ±135°, and ±45°. The measured output phase imbalances of filtering Butler matrix are within ± 12° in the passband. In the same way, the filter order of the Butler matrix could be extended by cascading more resonators at the input or output ports of the 180° filtering coupler. The normalized array factors for linear antenna array with eight elements have been calculated by using the measured phases and amplitudes of the Butler matrix at different frequency. Fig. 21 shows the theoretical and calculated array factors for the center frequency f_0 = 2.4 GHz with radiating elements' spacing equal to $0.5\lambda_0$. Close correlation has been found between the calculated array factors and the theoretical ones. Table IV lists the comparisons between the proposed Butler matrix and the previous work. It can be seen from the table that the proposed Butler matrix can provide a filtering function with more phase increments.

IV. Conclusion

This paper presents a systematic design process for the 4 × 4 and 8 × 8 filtering Butler matrices. The Butler matrices are composed of 180° filtering couplers based on coupled resonators, 90° directional couplers and phase shifters, which can realize different phase difference and equal power distribution as well a bandpass response. For validation, two examples of 4 × 4 and 8 × 8 filtering Butler matrices have been devised, manufactured, and measured. In addition, the normalized array factors were calculated based on the measured results to further indicate the acceptance of the measured results.

References

[1] T.-H. Lin, S.-K. Hsu, and T.-L. Wu, "Bandwidth enhancement of 4 × 4 Butler matrix using broadband forward-wave directional coupler and phase difference compensation," *IEEE Trans. Microw. Theory Techn.*, vol. 61, no. 12, pp. 4099–4109, Dec. 2013.

[2] J. Blass, "Multidirectionnal antenna, a new approach to stacked beams," *IRE Int. Conf. Record*, vol. 8, pt. 1, pp. 48–50, 1960.

[3] J. Nolen, "Synthesis of multiple beam networks for arbitrary illuminations," Ph.D. dissertation, The Johns Hopkins Univ., Baltimore, MD, 1965.

[4] P.-Z. Li, H. Ren, and B. Arigong, "A symmetric beam-phased array fed by a Nolen matrix using 180◦ couplers," *IEEE Microw. Wireless Compon. Lett.*, vol. 30, no. 4, pp. 387–390, Apr. 2020.

[5] H. Ren, H.-X. Zhang, Y.-Q. Jin, and B. Arigong, "A novel 2-D 3 × 3 Nolen matrix for 2-D beamforming applications," *IEEE Trans. Microw. Theory Techn.*, vol. 67, no. 11, pp. 4622-4631, Nov. 2019.

[6] T. Djerafi, N. Fonseca, and K. Wu, "Broadband substrate integrated waveguide 4 × 4 Nolen matrix based on coupler delay compensation," *IEEE Trans. Microw. Theory Techn.*, vol. 59, no. 7, pp. 1740-1745, Jul 2011.

[7] J. Butler and R. Lowe, "Beam-forming matrix simplifies design of electronically scanned antennas," *Electron. Design*, pp. 170–173, Apr. 1961.

[8] H. N. Chu and T.-G. Ma, "An extended 4 × 4 Butler matrix with enhanced beam controllability and widened spatial coverage," *IEEE Trans. Microw. Theory Techn.*, vol. 66, no. 3, pp. 1301–1311, Mar. 2018.

[9] A. Tajik, A. S. Alavijeh, and M. Fakharzadeh, "Asymmetrical 4 × 4 Butler matrix and its application for single layer 8 × 8 Butler matrix," *IEEE Trans. Antennas Propag.*, vol. 67, no. 8, pp. 5372–5379, Aug. 2019.

[10] H. M. Liu, S. J. Fang, Z. B. Wang, and S. Q. Fu, "Design of arbitrary-phase-difference transdirectional coupler and its application to a flexible Butler matrix," *IEEE Trans. Microw. Theory Techn.*, vol. 67, no. 10, pp. 4175–4185, Oct. 2019.

[11] H. Ren, P. Z. Li, Y. X. Gu, and B. Arigong, "Phase shifter-relaxed and control-relaxed continuous steering multiple beamforming 4 × 4 Butler matrix phased array," *IEEE Trans. Circuits Syst. I, Reg. Papers*, vol. 67, no. 12, pp. 5031–5039, Dec. 2020.

[12] N. Ashraf, A.-R. Sebak, and A. A. Kishk, "PMC packaged single-substrate 4 × 4 Butler matrix and double-ridge gap waveguide horn antenna array for multibeam applications," *IEEE Trans. Microw. Theory Techn.*, vol. 69, no. 1, pp. 248–261, Jan. 2021.

[13] E. T. Der, T. R. Jones, and M. Daneshmand, "Miniaturized 4×4 Butler matrix and tunable phase shifter *using* ridged half-mode substrate integrated waveguide," *IEEE Trans. Microw. Theory Techn.*, vol. 68, no. 8, pp. 3379-3388, Aug. 2020.

[14] H. Zhu, P.-Y. Qin, and Y. J. Guo, "Single-ended-to-balanced power divider with extended common-mode suppression and its application to differential 2×4 Butler matrices," *IEEE Trans. Microw. Theory Techn.*, vol. 68, no. 4, pp. 1510 - 1519, Apr. 2020.

[15] A. Tamayo-Domínguez, J.-M. Fernández-González, and M. Sierra-Castañer, "3-D-printed modified Butler matrix based on gap waveguide at W-band for monopulse radar," *IEEE Trans. Microw. Theory Techn.*, vol. 68, no. 3, pp. 926 - 938, Mar. 2020.

[16] T.-Y. Chin, J.-C. Wu, S.-F. Chang, and C.-C. Chang, "A V-band 8×8 CMOS Butler matrix MMIC," *IEEE Trans. Microw. Theory Techn.*, vol. 58, no. 12, pp. 3538–3546, Dec. 2010.

[17] B. Cetinoneri, Y. A. Atesal, and G. M. Rebeiz, "An 8×8 Butler matrix in 0.13-μm CMOS for 5–6-GHz multibeam applications," *IEEE Trans. Microw. Theory Techn.*, vol. 59, no. 2, pp. 295–301, Feb. 2011.

[18] K. Wincza, S. Gruszczynski, and K. Sachse, "Broadband planar fully integrated 8 × 8 Butler matrix using coupled-line directional couplers," *IEEE Trans. Microw. Theory Techn.*, vol. 59, no. 10, pp. 2441–2446, Oct. 2011.

[19] K. Wincza and S. Gruszczynski, "Broadband integrated 8 × 8 Butler matrix utilizing quadrature couplers and Schiffman phase shifters for multibeam antennas with broadside beam", *IEEE Trans. Microw. Theory Techn.*, vol. 64, no. 8, pp. 2596-2604, Aug. 2016.

[20] V. T. Crestvolant, P. M. Iglesias, and M. J. Lancaster, "Advanced Butler matrices with integrated bandpass filter functions," *IEEE Trans. Microw. Theory Techn.*, vol. 62, no. 11, pp. 2659–2672, Nov. 2014.

[21] Q. Shao, F. C. Chen, Q. X. Chu, and M. J. Lancaster, "Novel filtering 180° hybrid coupler and its application to 2 × 4 filtering Butler matrix," *IEEE Trans. Microw. Theory Techn.*, vol. 66, no. 7, pp. 3288–3296, Jul. 2018.

[22] J. Allen, "A theoretical limitation on the formation of lossless multiple beams in linear arrays," *IEEE Trans. Antennas Propag.*, vol. 9, no. 4, pp. 350–352, Jul. 1961.

[23] H. Moody, "The systematic design of the Butler matrix," *IEEE Trans. Antennas Propag.*, vol. 12, no. 6, pp. 786–788, Nov. 1964.

[24] D. M. Pozar, *Microwave Engineering*, 3RD ed. New York: Wiley, 2005.

[25] T. Macnamara, "Simplified design procedures for Butler matrices incorporating 90° hybrids or 180° hybrids," *Proc. Inst. Elect. Eng.—Microw., Antennas Prop.*, vol. 134, no. 1, pt. H, pp. 50–54, 1987.

[26] R. Gómez-García, L. Yang, J.-M. Muñoz-Ferreras, and D. Psychogiou, "Single/multi-band coupled-multi-line filtering section and its application to RF diplexers, bandpass/bandstop filters, and filtering couplers," *IEEE Trans. Microw. Theory Techn.*, vol. 67, no. 10, pp. 3959–3972, Oct. 2019.

[27] M. F. Hagag, M. A. Khater, M. D. Sinanis, and D. Peroulis, "Ultra-compact tunable filtering rat-race coupler based on half-mode SIW evanescent-mode cavity resonators," *IEEE Trans. Microw. Theory Techn.*, vol. 66, no. 12, pp. 5563–5572, Dec. 2018.

[28] F. Lin and H.-Z. Ma, "Design of a class of filtering couplers with reconfigurable frequency," *IEEE Trans. Microw. Theory Techn.*, vol. 66, no. 9, pp. 4017–4028, Sep. 2018.

[29] C.-K. Lin and S.-J. Chung, "A compact filtering 180 hybrid," *IEEE Trans. Microw. Theory Techn.*, vol. 59, no. 12, pp. 3030–3036, Dec. 2011.

[30] X. Zhu, T. Yang, P. L. Chi, and R. M. Xu, "Novel reconfigurable filtering rat-race coupler, branch-line coupler, and multiorder bandpass filter with frequency, bandwidth, and power division ratio control," *IEEE Trans. Microw. Theory Techn.*, vol. 68, no. 4, pp. 1496–1509, Apr. 2020.

[31] W. Yu, Y. B. Rao, H. Z. J. Qian, and X. Luo, "Reflectionless filtering 90° coupler using stacked cross coupled-line and loaded cross-stub," *IEEE Microw. Wireless Compon. Lett.*, vol. 30, no. 5, pp. 481–484, May. 2020.

[32] G. Zhang, F. Jiao, S. C. Liu, L. Zhu, S. Y. Wang, Q. Y. Zhang, and J. Q. Yang, "Compact single- and dual-band filtering 180°_hybrid couplers on circular patch resonator," *IEEE Trans. Microw. Theory Techn.*, vol. 68, no. 9, pp. 3675–3685, Sep. 2020.

[33] H.-Y. Li, J.-X. Xu, and X. Y. Zhang, "Substrate integrated waveguide filtering rat-race coupler based on orthogonal degenerate modes," *IEEE Trans. Microw. Theory Techn.*, vol. 67, no. 1, pp. 140–150, Jan. 2019.

[34] Q. Shao, F. C. Chen, Y. Wang, Q. X. Chu, and M. J. Lancaster, "Design of modified 4 × 6 filtering Butler matrix based on all-resonator structures," *IEEE Trans. Microw. Theory Techn.*, vol. 67, no. 9, pp. 3617–3627, Sep. 2019.

[35] S. Gruszczynski, K. Wincza, and K. Sachse, "Design of compensated coupled-stripline 3-dB directional couplers, phase shifters, and magic-T's—Part I: Single-section coupled-line circuits," *IEEE Trans. Microw.* Theory Techn., vol. 54, no. 11, pp. 3986–3994, Nov. 2006.

Qiang Shao was born in Xianning, Hubei Province, China, in January 1993. He received the B.S. degree in information engineering from Shantou University, Shantou, Guangdong, China in 2015. He is currently working towards the Ph.D. degree at South China University of Technology. His research interests include microwave filters and associated RF circuits for microwave and millimeter-wave applications.

Fu-Chang Chen (M'12) was born in Fuzhou, Jiangxi Province, China, in December 1982. He received the Ph.D. degree from South China University of Technology, Guangzhou, Guangdong, China, in 2010. He is currently a Professor with the School of Electronic and Information Engineering, South China University of Technology. His research interests include the synthesis theory and design of microwave filters and associated RF modules for microwave and millimeter-wave applications.

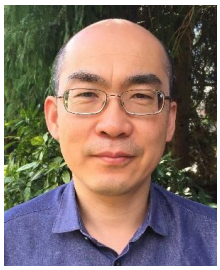

Yi Wang (M'09–SM'12) was born in Shandong, China. He received the B.Sc. degree in applied physics and M.Sc. degree in condensed matter physics from the University of Science and Technology, Beijing, China, in 1998 and 2001, respectively, and the Ph.D. degree in electronic and electrical engineering from the University of Birmingham, Edgbaston, Birmingham, U.K., in 2005.

From 2004 to 2011, he was a Research Fellow at the University of Birmingham. In 2011, he became a Senior Lecturer and then Reader at the University of Greenwich, U.K.. He is currently an Associate Professor with the University of Birmingham. He is the author of over 160 research papers. He has been the reviewer of several major microwave, antenna and sensor journals and Associate Editor of IET MAP. He serves the TPC Chair of 2021 European Microwave Conference. His current research interests include multiport filtering networks, filter-antenna integration, millimeter-wave and terahertz antennas and devices for metrology, communication, and sensing. He is particularly interested in working with new materials and various novel manufacturing techniques, such as micromachining and 3D printing, for RF/microwave applications.

Qing-Xin Chu (M'99–SM'11–F'18) received the B.S., M.E., and Ph.D. degree in electronic engineering from Xidian University, Xi'an, Shaanxi, China, in 1982, 1987, and 1994, respectively.

He is currently a chair professor with the School of Electronic and Information Engineering, South China University of Technology. He is also the director of the Research Institute of Antennas and RF Techniques of the university, the chair of the Engineering Center of Antennas and RF Techniques of Guangdong Province. He is also with Xidian University as a distinguished professor in Shaanxi Hundred-Talent Program since 2011. From Jan. 1982 until Jan. 2004, he was with the School of Electronic Engineering, Xidian University, and since 1997, he was a professor and the vice dean of the School of Electronic Engineering, Xidian University.

He is the foundation chair of IEEE Guangzhou AP/MTT Chapter and a Fellow of the Chinese Institute of Electronics (CIE). He has published over 300 papers in journals and conferences, which were indexed in SCI more than 1500 times. One of his papers published in IEEE Transactions on Antennas and Propagations in 2008 becomes the top ESI (Essential Science Indicators) paper within 10 years in the field of antenna (SCI indexed self-excluded in the antenna field ranged top 1%). In 2014, he was elected as the highly cited scholar by Elsevier in the field of Electrical and Electronic Engineering. He has authorized more than 30 invention patents of China.

He was the recipient of the Science Award by Guangdong Province in 2013 , the Science Awards by the Education Ministry of China in 2008 and 2002, the Fellowship Award by Japan Society for Promotion of Science (JSPS) in 2004, the Singapore Tan Chin Tuan Exchange Fellowship Award in 2003, the Educational Award by Shaanxi Province in 2003.